Structure of $Ca(BD_4)_2$ β-Phase from Combined Neutron and Synchrotron X-ray Powder Diffraction Data and Density Functional Calculations

F. Buchter,*,†,▽ Z. Łodziana,† A. Remhof,† O. Friedrichs,† A. Borgschulte,† Ph. Mauron,† A. Züttel,†,▽ D. Sheptyakov,‡ G. Barkhordarian,§ R. Bormann,§ K. Chłopek,|| M. Fichtner,|| M. Sørby,⊥ M. Riktor,⊥ B. Hauback,⊥ and S. Orimo#

Empa, Laboratory for Hydrogen & Energy, Swiss Federal Laboratories for Materials Testing and Research, Überlandstrasse 129, CH-8600 Dübendorf, Switzerland, Laboratory for Neutron Scattering, ETH Zurich & Paul Scherrer Institute, CH-5232 Villigen PSI, Switzerland, GKSS-Research Center Geesthacht GmbH, WTP, Building 59, Max-Planck-Strasse 1, 21502 Geesthacht, Germany, Institute of Nanotechnology, Forschungszentrum Karlsruhe, P.O. Box 3640, D-76021 Karlsruhe, Germany, Institute for Energy Technology, P.O. Box 40, NO-2027 Kjeller, Norway, and Institute for Materials Research, Tohoku University, 980-8577 Sendai, Japan

Received: January 16, 2008; Revised Manuscript Received: April 2, 2008

We have investigated the crystal structure of $Ca(BD_4)_2$ by combined synchrotron radiation X-ray powder diffraction, neutron powder diffraction, and ab initio calculations. $Ca(BD_4)_2$ shows a variety of structures depending on the synthesis and temperature of the samples. An unknown tetragonal crystal of $Ca(BD_4)_2$, the β phase has been solved from diffraction data measured at 480 K on a sample synthesized by solid−gas mechanochemical reaction by using MgB_2 as starting material. Above 400 K, this sample has the particularity to be almost completely into the β phase of $Ca(BD_4)_2$. Seven tetragonal structure candidates gave similar fit of the experimental data. However, combined experimental and ab initio calculations have shown that the best description of the structure is with the space group $P4_2/m$ based on appropriate size/geometry of the (BD_4) tetrahedra, the lowest calculated formation energy, and real positive vibrational energy, indicating a stable structure. At room temperature, this sample consists mainly of the previously reported α phase with space group *Fddd*. In the diffraction data, we have identified weak peaks of a hitherto unsolved structure of an orthorombic γ phase of $Ca(BD_4)_2$. To properly fit the diffraction data used to solve and refine the structure of the β phase, a preliminar structural model of the γ phase was used. A second set of diffraction data on a sample synthesized by wet chemical method, where the γ phase is present in significant amount, allowed us to index this phase and determine the preliminar model with space group *Pbca*. Ab initio calculations provide formation energies of the α phase and β phase of the same order of magnitude ($\Delta H \leq 0.15$ eV). This indicates the possibility of coexistence of these phases at the same thermodynamical conditions.

I. Introduction

Because of their high volumetric and gravimetric hydrogen density, alkali and earth alkali p-element complex hydrides attract a growing interest as hydrogen storage materials[1–3] (gravimetric density of hydrogen up to 20 mass% and high volumetric density up to 150 kg m^{-3}). $Ca(BH_4)_2$, with a gravimetric hydrogen density of 11.5 mass% and a volumetric hydrogen density of ∼130 kg m^{-3}, is among the most promising compounds for hydrogen storage. Research on $Ca(BH_4)_2$ is currently focused on physical properties of the compound[4–8] as well as on the synthesis.[4,6] Despite their high heat of formation, reflected in high stabilities, borohydrides do not form easily from the elements. To overcome the kinetic barrier of formation, appropriate catalysts or reactants have to be found. It has been shown recently that MgB_2 is such a suitable reactant for the formation of $Li(BH_4)$, $Na(BH_4)$, and $Ca(BH_4)_2$.[4] In the reaction $CaH_2 + MgB_2 + 4H_2 \rightarrow Ca(BH_4)_2 + MgH_2$, theoretically, 8.3 wt% hydrogen can be absorbed.[4] In situ synchrotron radiation X-ray powder diffraction (SR-XPD) studies focused on both phase transitions and decomposition routes on samples synthesized by different methods that have been recently published.[5,8] The decomposition of $Ca(BH_4)_2$, synthesized by solid−gas mechanochemical reaction with MgB_2 as starting material,[4] starts above 603 K. forming CaH_2, $Ca_3Mg_4H_{14}$, Mg, B, and H_2 till complete decomposition into CaH_2, Mg, B, and H_2 above 673 K.[5] A similar decomposition scheme was observed for $Ca(BH_4)_2$ synthesized by the wet chemical method,[6] differing only for the first decomposition step where no $Ca_3Mg_4H_{14}$ is observed but rather some amount of more stable high-temperature phases of $Ca(BH_4)_2$.[8]

Depending on the synthesis and the temperature of the samples, $Ca(BH_4)_2$ can assume a variety of crystal structures, which are to a large extent still unknown and under investigation.[9,10] A room temperature (RT), orthorombic crystal structure of $Ca(BH_4)_2$ with space group *Fddd* (no. 70) named the α phase[5,8] was recently determined.[7] The $Ca(BH_4)_2$ sample was obtained by drying a commercially available complex $Ca(BH_4)_2 \cdot 2THF$. In our data, the diffraction pattern of $Ca(BD_4)_2$ synthesized by solid−gas mechanochemical reaction with MgB_2 as starting

* Corresponding author. E-mail: florian.buchter@empa.ch.
† Swiss Federal Laboratories for Materials Testing and Research.
‡ ETH Zurich & Paul Scherrer Institute.
§ GKSS-Research Center Geesthacht GmbH.
|| Forschungszentrum Karlsruhe.
⊥ Institute for Energy Technology.
Tohoku University.
▽ Also at University of Fribourg, Physics Department, CH-1700 Fribourg, Switzerland.

10.1021/jp800435z CCC: $40.75
Published on Web 06/14/2008

TABLE 1: Summary of the Measured Samples, Used Instrument, Measurment Conditions, and Use of the Diffraction Data

use[a]	phase	sample	radiation/instrument	T (K)	λ (Å)
I	β	$Ca(BD_4)_2 + MgD_2$	SR-XPD/SNBL-B	90, 300, 480	0.49983
I	β	$Ca(BD_4)_2 + MgD_2$	SR-XPD/ID31	300, 480	0.80007
S, R	β, α	$Ca(^{11}BD_4)_2 + MgD_2$	SR-XPD/SLS-MS	300, 480	0.95487
S, R	β, α	$Ca(^{11}BD_4)_2 + MgD_2$	NPD/HRPT	300, 480	1.49255
I	γ	$Ca(BH_4)_2$	SR-XPD/SNBL-B	300, 480	0.49895
S, R	γ	$Ca(BD_4)_2$	SR-XPD/SLS-MS	300	0.95487
S, R	γ	$Ca(BD_4)_2$	NPD/HRPT	300	1.88489

[a] I, Indexation; S, solution; R, refinement.

material shows peaks of the RT α phase coexisting with minor peaks of a hitherto unsolved orthorombic structural phase with space group *Pbca* (no. 61), the so-called γ phase.[8] The α phase transforms at about 400 K to an hitherto unknown tetragonal structural phase with space group $P4_2/m$ (no. 84) called the β phase.[5,8] In the diffraction pattern at 480 K, intense peaks of β phase are observed, whereas only very weak peaks of α phase and γ phase are observed. Peaks of $Ca_3Mg_4D_{14}$ with significant intensity and peaks of the MgB_2 byproduct are observed at RT and at 480 K. The diffraction patterns of $Ca(BH_4)_2$ synthesized by the wet chemical method show peaks of similar intensity from both the γ phase and the β phase in the temperature range from RT up to 600 K and weaker peaks of the α phase. The intensity of the peaks belonging to the α phase is however significant and depends on the synthesis conditions.

In the present work, we have investigated and solved the crystal structure of the β phase of $Ca(BD_4)_2$ by combined X-ray and neutron diffraction. Samples of $Ca(BD_4)_2 + MgD_2$ prepared by solid−gas mechanochemical reaction were employed. These samples are especially suited because they contain predominantly the β phase above 400 K. The structure solution of the β phase can therefore be carried out, even with the weak contribution of the γ phase in the diffraction pattern. The final refinements of the β phase was performed by including a preliminary structural model of the γ phase. The γ phase was indexed by using data measured on $Ca(BH_4)_2$ and $Ca(BD_4)_2$ samples synthesized from the wet chemical method. In these samples, the γ phase is present in significant amount. Detailed structural analysis of the γ phase will be published in a forthcoming paper. We have investigated the α phase of $Ca(BD_4)_2$ by combined X-ray and neutron diffraction at RT, confirming the structure recently reported[7] for the corresponding hydride. We have performed density functional calculations of the formation energy and the normal-mode frequencies of all the α phase and the β phase of $Ca(BD_4)_2$. The similar range of the energy of formation of all the considered phases (within ~0.15 eV) explains the coexistence at the same thermodynamic conditions of the α phase and the β phase in varrying ratios in the $Ca(BD_4)_2$ sample synthesized by the wet chemical method.

II. Methods

A. Experimental Section. ***1. Samples Synthesis.*** For the identification and indexing of the β phase, a sample of $Ca(BD_4)_2 + MgD_2$ prepared by solid−gas mechanochemical reaction[4] at the GKSS Research Center, Geesthacht, Germany, was employed. The sample was synthesized by the solid−gas reaction of MgB_2 and CaD_2 at 673 K and 350 bar of D_2.[4] MgB_2 (−325 mesh powder) was purchased from Alfa-Aesar, and CaD_2 was synthesized by reaction of Ca (98%, Mg < 1%, Alfa-Aesar) with deuterium at 50 bar and 573 K. Mixtures of CaD_2 and Mg_2 (1:1 molar) were milled for 90 min in a Spex 8000 M mill under Argon, with a ball-to-powder ratio of 10. In order to avoid the high neutron absorption of natural boron for neutron diffraction measurements, a second sample containing $Ca(^{11}BD_4)_2 + MgD_2$ with isotope 11 of boron was synthesized at the GKSS by the same procedure[4] $Mg^{11}B_2$ was synthesized by heating a milled (Spex 8000, 90 min) mixture of MgD_2 (Th. Goldschmidt AG) and isotope 11 of boron (isotopic enrichment 99.65%, chemical purity >99.63%, Cambridge Isotopes Laboratories Inc.), first to 623 K for 6 h (under vacuum) and then to 873 K for 24 h under argon.

For the indexing of the crystal structure of the γ phase, a sample of $Ca(BH_4)_2$ was synthesized by wet chemical synthesis[6] at the Forschungszentrum Karlsruhe GmbH, Germany. For the synthesis, 1.920 g (0.046 mol) of CaH_2 was purchased from Aldrich (purity 99.9%) and introduced to 15.743 g (0.137 mol) of $Et_3N{\cdot}BH_3$ purchased from Aldrich. Isolated yield was 2.690 g (85%). Elemental analysis showed 10.45% H (theor., 11.56% H). For the solution and refinement of the preliminary structural model of the γ phase, a sample of $Ca(BD_4)_2$ was synthesized by wet chemical synthesis.[6] The compound was synthesized with a yield of 84% from 1.046 g (0.024 mol) of synthesized[11] CaD_2 and 6.161 g (0.052 mol) of synthesized $Et_3N{\cdot}BD_3$. The latter compound was prepared from $NaBD_4$ (Alfa Aesar, 9.500 g, 0.227 mol) and triethylamine-hydrochloride salt (Merck, 28.399 g, 0.206 mol) in diethyl ether[12] with a total yield of 87%. Because of the rapid solidification of the $Ca(BD_4)_2$, the final compound contains several percent of unreacted CaD_2. Isolated yield was 2.690 g (85%). Elemental analysis showed 10.42% D (theor., 11.56% D).

All samples were handled exclusively in vacuum or in inert gas prior to filling into glass capillaries or sample containers used for the diffraction measurements. Table 1 gives a summary of the measured samples, the corresponding measurement conditions, and the use of the data. The indexing of the β phase and the γ phase was carried out by using SR-XPD. Solution and final refinements of the β phase and the α phase as well as preliminar study of the γ phase structure were performed by using combined SR-XPD and neutron powder diffraction (NPD) data (see Figure 1).

2. Indexing. For the indexing of the β phase, SR-XPD data for the sample of $Ca(BD_4)_2 + MgD_2$ was collected at 90, 300, and 480 K on the high-resolution powder diffractometer of the Swiss-Norwegian beamlines (BM01B-SNBL) and at 300 and 480 K at the high-resolution powder diffraction beamline (ID31) at the European Synchrotron Radiation Facility (ESRF) in Grenoble (France). The sample was filled into 0.8 mm diameter glass capillaries for the measurements at SNBL and into a 1.0 mm diameter glass capillary at ID31. The wavelength was 0.499830 Å at SNBL and 0.800016 Å at ID31. In both cases, the temperature was controlled by using an Oxford Cryostream 600 blower. Measurements at different temperatures (above and below the transition from α phase to β phase at ~400 K) and on two different instruments allowed to identify the shift or appearance/disappearence of diffraction peaks due to thermal expansion or phase transitions. It allowed to attribute the peaks

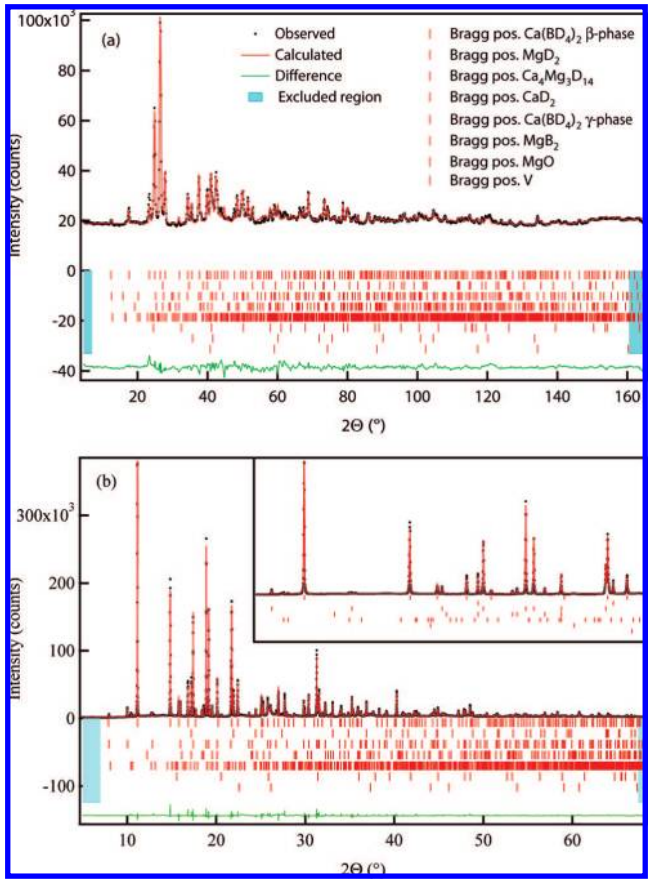

Figure 1. Result of combined NPD (a) and SR-XPD (b) Rietveld refinement of the $Ca(BD_4)_2$ β phase by using diffraction patterns measured on the $Ca(^{11}BD_4)_2 + MgD_2$ sample at 480 K. Rows of Bragg-peak positions follow the order of the corresponding legend in panel a.

to the different structural phases of $Ca(BD_4)_2$, the byproduct MgD_2, and impurity phases. For the indexing of the γ phase, SR-XPD data on the sample of $Ca(BD_4)_2$ was collected at 300 and 480 K with the high-resolution powder diffractometer BM01B at SNBL. The sample was filled into a 0.8 mm diameter glass capillary, and the wavelength was 0.499830 Å. For the same reasons as those mentioned for the β phase, measuring the γ phase at two temperatures allowed to identify the peaks belonging to the different structural phases of $Ca(BH_4)_2$ and impurity phases. The indexing by using the fitted position of the identified peaks of each phases was performed by using the program Dicvol04.[13] The β phase was found to be tetragonal, and the refined unit cell parameters are listed in Table 2. The γ phase was found to be orthorombic with refined unit cell parameters a = 13.0582(3) Å, b = 8.3882(5) Å, and c = 7.5108(4) Å.

3. Solution and Refinement. For the solution and refinement of the β phase (respectively, refinement of the α -phase), SR-XPD data on the sample of $Ca(^{11}BD_4)_2 + MgD_2$ were collected at 480 K (respectively, 300 K) on the high-resolution powder diffractometer of the material science (MS) beamline at the Swiss Light Source (SLS) at the Paul Scherrer Institute (PSI) in Villigen (Switzerland). For the solution and preliminar refinement of the γ phase, SR-XPD data on the sample of $Ca(BD_4)_2$ was collected at 300 K on the MS beamline at the SLS. Both samples were measured in the same conditions. They were filled into 1.0 mm diameter glass capillary, the wavelength was 0.954872 Å, and the temperature was controlled by an Oxford Cryostream 600 blower. NPD data were collected on

TABLE 2: Refined Structural Parameters of the β Phase

site	x/a	y/b	z/c	B_{iso} (Å^2)
Space Group $P4_2/m$ (no. 84); $Z = 2$				
Experimental; T = 480 K; a = 6.9468(1) Å, c = 4.3661(1) Å				
Ca/2c	0.5	0	0.5	3.9(2)
B/4j	0.302(4)	0.200(5)	0	3.3(4)
D1/4j	0.295(8)	0.347(9)	0	11.0(11)
D2/4j	0.468(7)	0.185(5)	0	11.0(11)
D3/8k	0.226(5)	0.161(5)	0.800(6)	11.0(11)
Calculated; a = 7.1160 Å, c = 6.6730 Å				
Ca/2c	0.5	0	0.5	
B/4j	0.3146	0.2183	0	
D1/4j	0.3264	0.4017	0	
D2/4j	0.4909	0.1657	0	
D3/8k	0.2243	0.1560	0.7704	
Space Group $P4_2$ (no. 77); $Z = 2$				
Experimental; T = 480 K; a = 6.9468(11) Å, c = 4.3661(8) Å				
Ca/2c	0	0.5	0	3.9(2)
B/4d	0.207(5)	0.699(5)	0.534(11)	2.8(4)
D1/4d	0.355(8)	0.728(11)	0.61(2)	9.7(10)
D2/4d	0.148(9)	0.734(8)	0.29(2)	9.7(10)
D3/4d	0.173(11)	0.827(9)	0.71(2)	9.7(10)
D4/4d	0.184(5)	0.553(8)	0.48(2)	9.7(10

the $Ca(^{11}BD_4)_2 + MgD_2$ sample at 300 and 480 K for the solution and final refinements of the β phase and on the $Ca(BD_4)_2$ sample at 300 K for the solution and preliminar refinement of the γ phase. The data were collected at the high-resolution powder diffractometer for thermal neutrons[14] (HRPT) at the Swiss spallation neutron source (SINQ) at the PSI. The powder of $Ca(^{11}BD_4)_2 + MgD_2$ was filled into a vanadium cylinder of 6 mm inner diameter and 50 mm length. Diffraction patterns were recorded with monochromatic neutrons of wavelength of 1.492546 Å for the $Ca(^{11}BD_4)_2 + MgD_2$ sample. The absorption correction coefficient of the sample $\mu R = 0.158$ was determined by transmission measurements. The powder of $Ca(BD_4)_2$ was filled into a double-walled vanadium cylinder of 9 mm outer diameter, 7 mm inner diameter, and 50 mm length. Diffraction patterns were recorded with monochromatic neutrons of wavelength of 1.884886 Å for the $Ca(BD_4)_2$ sample. The absorption correction coefficient $\mu R = 0.296$ was determined by transmission measurements. The temperature control of both samples was realized by means of a small furnace mounted into an evacuated aluminum vessel.

The structure solution of the β phase (respectively, γ phase) was performed by the program FOX[15] (version 1.7.0) by using combined SR-XPD and NPD data. The space-group candidates were determined by a systematical profile matching of the data with all the possible tetragonal space groups and orthorombic space groups, respectively, considering all the permutations of lattice vectors. FOX was run for all the space-group candidates fitting all the indexed β-phase peaks (respectively, γ-phase peaks). For the β phase, the atomic positions found by FOX resulted in (BD_4) tetrahedron with physically realistic interatomic distances for eight structural models corresponding to the space groups listed in Table 4 and represented in Figure 2. For the γ phase, the space group *Pbca* (no. 61) was considered because this space group is the only one of higher symmetry yielding (BD_4) tetrahedra with physically realistic interatomic distances.

The combined SR-XPD and NPD refinement of the structural models was carried out by using the program FullProf[16] (version 3.80). For the β phase, all the refined structural model candidates were found to give equivalent quality of fit for both neutron and X-ray pattern except for the space group $P4_2/mnm$ (no. 136)

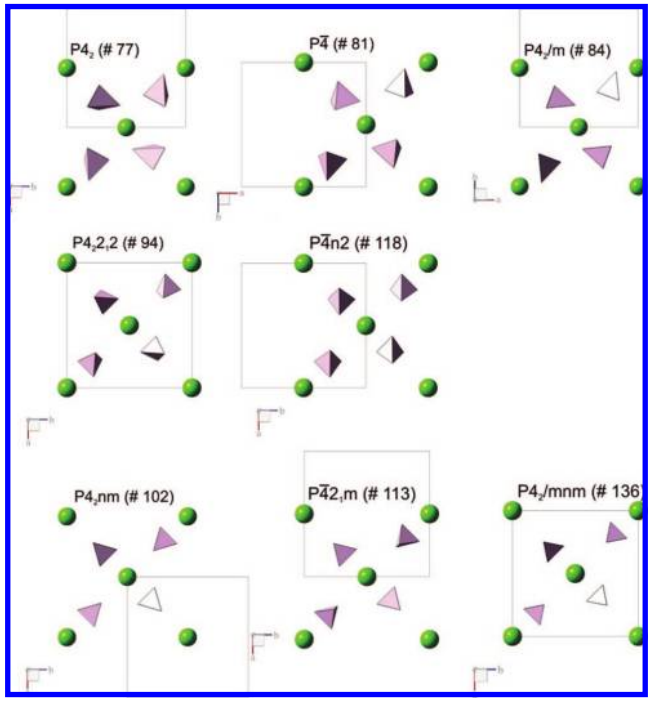

Figure 2. Structure of refined experimental $Ca(BD_4)_2$ β-phase models viewed in the plane (001). The space group number of each model is indicated. To emphasize the similarity of the Ca−B networks for the different structures, only the BD_4 shape is drawn, and the atoms are not necessarily represented in the conventional unit cell (drawn by black frames) but in a cell shifted along the *a* and/or *b* axis.

with worse Rwp values for the neutron data (see Table 4.). The models fitted in the space groups $P4_2$ (no. 77) and $P4_2/m$ (no. 84) have (BD_4) tetrahedra of the expected size (B−D distances not lower than 1.1 Å) and thermal displacement parameters approximately half of the ones obtained for the other structural models. All the other structural models show at least one too-short boron−deuterium distance and large displacement parameters (see Table 4.). For the α-phase of $Ca(BD_4)_2$, the atomic positions of the recently reported structural model[7] are compatible with our data and were used as initial values for the final refinement. Scattering form factors and scattering length from the FullProf library were used, except for the scattering length of the isotope 11 of boron, where a value of 6.65 fm was introduced.[17] A weight of 0.9 for the NPD data and 0.1 for the SR-XPD data was given in the combined refinement.

Details of the refined structural model with space group $P4_2/m$ and $P4_2$ of the β phase of $Ca(BD_4)_2$ are given in Table 2. The final refinement of the β-phase structural model with space group $P4_2/m$ (see Figure 1) was done with 87 free parameters (respectively, 93 for the model with space group $P4_2$ because of a different number of atomic positions). Two unit cell parameters, nine atomic positions (respectively, 15 for the model with space group $P4_2$), and three isotropic displacement parameters were refined (all D atoms are constrained to have the same displacement parameters). All the structural parameters were refined without imposing any restraints on bond lengths or angles. Six other phases were also refined to account for byproduct, other $Ca(BD_4)_2$ phases, and impurities identified in the diffraction pattern (MgD_2, $Ca_4Mg_3D_{14}$, CaD_2, $Ca(BD_4)_2$ γ phase, MgB_2, and MgO), and an additional seventh phase (vanadium) was refined only for the NPD data to take into account the diffraction of the sample holder. For these seven phases, a total of 39 structural parameters (unit cell, atomic positions, and displacement parameters) were refined. Thomson−Cox−Hastings modified pseudo-Voigt profile functions were used to model the peak shape for both SR-XPD and NPD diffraction patterns. For the SR-XPD data, the instrumental profile parameters (*U* and *V*) were refined by the fitting of data measured on a NAC standard. The sample profile parameters were fixed by a profile matching of the SR-XPD data. The instrumental and sample profile parameters for the SR-XPD data were kept fixed at these values for the final refinement. For the NPD data profile, four profile parameters were used in the final refinement. In addition, two zero-shift paramaters, neutron wavelength, and 15 scale factors were refined. The modeling of the background was done by a 12-refined-coefficients Fourier-cosine series for the NPD data and an interpolation between 42 fixed points for the SR-XPD data.

TABLE 3: Refined Structural Parameters of the α Phase

Space Group *Fddd* (no. 70, Setting 2); $Z = 8$				
site	*x*/*a*	*y*/*b*	*z*/*c*	B_{iso} (Å^2)
$T = 300$ K; $a = 8.7461(8)$ Å, $b = 13.0942(9)$ Å, $c = 7.4660(7)$ Å				
Ca/8a	0.125	0.125	0.125	2.0(2)
B/16f	0.125	0.345(1)	0.125	1.7(4)
D1/32 h	0.018(2)	0.399(2)	0.113(4)	4.4(4)
D2/32 h	0.126(3)	0.298(2)	0.257(3)	4.4(4)

Details of the refined structural model of the α phase of $Ca(BD_4)_2$ are given in Table 3. The final refinement (see Figure 5) was done with 86 refined parameters. Three unit cell parameters, seven atomic positions, and three isotropic displacement parameters were used. All atoms of the same species were constrained to have the same displacement parameters. All structural parameters were refined without applying any restraint on bond lengths or angles. Six other phases were also refined to account for other $Ca(BD_4)_2$ phases and impurities identified in the diffraction pattern ($Ca(BD_4)_2$ γ phase, MgD_2, $Ca_4Mg_3D_{14}$, CaD_2, MgB_2, MgO), and an additional seventh phase (vanadium) was refined only for the NPD data to take into account the diffraction of the sample holder. In total, 44 structural parameters (unit cell, atomic positions, and displacement parameters) were refined for these seven phases. For the peak shape, Thomson−Cox−Hastings modified pseudo-Voigt profile functions were used for both SR-XPD and NPD diffraction patterns. The same procedure as that used to determine the parameters of the β-phase profile function of the SR-XPD data was applied. For the NPD data profile, four profile parameters were used in the final refinement. In addition, two zero-shift parameters, neutron wavelength, and 15 scale factors were refined. The modeling of the background was done by a 12-refined-coefficients Fourier-cosine series for the NPD data and an interpolation between 24 fixed points for the SR-XPD data.

B. Theoretical Section. The structure and the normal-mode analysis of $Ca(BH_4)_2$ were calculated within density functional theory.[18] The elements were represented by projected augmented plane-wave[19,20] approach,[21] with the electronic configuration of $1s^1$ for H, $2s^22p^1$ for B, and $2s^2$ for Ca. The calculations were carried out within the generalized gradient approximation and the PW91[22] exchange correlation functional with a kinetic energy cutoff of 400 eV. The wave functions were sampled according to a Monkhorst−Pack scheme with a *k*-point mesh of spacing 0.07 Å^{-1}. The ground-state electronic density was determined by iterative diagonalization of the Kohn−Sham Hamiltonian. All considered structures were optimized with constrained symmetry until the forces excerced on atoms were smaller than 0.01 eV/Å. Then, the shape and volume of the unit cell was relaxed, and the procedure was repeated until self-consistency was achieved. In the last step, the symmetry

TABLE 4: Summary of Selected Structural Properties at $T = 480$ K, Calculated Formation-Energy Difference with Respect to the α Phase (*Fddd*), and Calculated Nature of Vibrational Frequencies of the Tetragonal Structure Candidates for the β Phase of $Ca(BD_4)_2$

space group	Rwp[a] NPD	Rwp[a] SR-XPD	B−D (Å)	$(\overline{B-D})$ (Å)	B_{iso}(D) (Å ^{2})	ΔE (eV/Å^3)[b]	ΔH (eV/Å^3)[c]	Frequ.[d]
$P4_2$	3.04	8.17	1.06(3)−1.20(4)	1.14(8)	9.7(10)	0.159	0.142	$\mathscr{R}$
$P\bar{4}$	2.97	8.46	0.83(5)−1.24(4)	1.04(9)	9.7(10)			
$P4_2/m$	3.27	8.19	1.02(3)−1.16(3)	1.07(5)	11.0(11)	0.151	0.134	$\mathscr{R}$
$P4_2/m$[e]	3.28	8.59	1.02(3)−1.16(3)	1.07(5)	11.0(11)			
$P4_22_12$	3.35	8.52	0.81(2)−0.90(3)	0.86(7)	18(2)	0.256		
$P4_2nm$	3.30	8.50	0.81(2)−1.01(5)	0.88(8)	17(2)	0.239		$\mathscr{T}$
$P\bar{4}2_1m$	3.35	8.53	0.66(5)−1.13(5)	0.87(8)	17(2)	0.162		
$P\bar{4}n2$	3.24	8.49	0.87(2)−1.00(2)	0.93(5)	15(2)	0.223		$\mathscr{T}$
$P4_2/mnm$	4.24	8.74	0.79(2)−0.791(20)	0.79(3)	8(2)	0.358		$\mathscr{T}$
Fddd						0	0	$\mathscr{R}$

[a] Weighted profile factor. [b] Electronic contribution of the formation-energy difference with respect to α phase. [c] Formation-energy difference including zero-point energy with respect to α phase. [d] $\mathscr{R}$, all calculated vibrational modes are real numbers. $\mathscr{T}$, some calculated vibrational modes are imaginary numbers. [e] Without considering the γ phase for the refinement.

constraints were removed and internal atomic positions were relaxed. This step showed that the structures were in local minima.

After this step, the normal-mode analysis was performed by finite displacement method of the symmetry inequivalent atoms. Each ion was displaced by 0.02 Å in two opposite directions along all crystallographic axes, and the dynamical matrix was constructed. The diagonal elements of the dynamical matrix represent normal modes at the gamma point. The zero-point vibration energy was calculated within harmonic approach; details are presented elsewhere.[23]

III. Results and Discussion

The structure of the β phase for $Ca(BD_4)_2$ was solved in spite of the multiphase nature of the sample because of two main reasons. First, at 480 K, the samples synthesized by solid−gas mechanochemical reaction consist almost completely of the β-phase form (see inset in Figure 1). This allows to solve the β phase without treating more than one unsolved structural phase of $Ca(BD_4)_2$ at the time. In the final refinement of the β phase, the structure of the γ phase of $Ca(BD_4)_2$ was introduced because small amounts of this phase were identified in the diffraction pattern (see inset of Figure 1). However, the γ-phase contribution to the diffraction pattern is minor as it can be seen in the inset of Figure 1 or by considering the reliability factors of the final refinement of the β phase with and without including the γ phase (see Table 4). Second, the use of high-resolution SR-XPD data reduced the peak overlapp and allowed the identification of all the peaks of the pattern (only few impurity peaks of very low intensity were not indexed in Figure 1).

A. Tetragonal β-Phase Structure of $Ca(BD_4)_2$. Seven tetragonal structural model candidates were identified for the hitherto unsolved tetragonal β structural phase (with corresponding space groups $P4_2$ (no. 77), $P\bar{4}$ (no. 81), $P4_2/m$ (no. 84), $P4_22_12$ (no. 94), $P4_2nm$ (no. 102), $P\bar{4}2_1m$ (no. 113), and $P\bar{4}n2$ (no. 118)). All candidates show nearly identical relative Ca and B positions (see Figure 2) and give roughly the same goodness of fit (see Table 4). They differ mainly in D positions or alternatively in (BD_4) orientation, sizen and distortion (see Figure 2 and Table 4). Space groups no. $P4_22_12$, $P4_2nm$, $P\bar{4}2_1m$, $P\bar{4}n2$, and $P4_2/mnm$ have diagonal, horizontal, or vertical mirror planes and/or screw axis parallel to the (001) plane imposing particular orientations of the (BD_4). For example $P4_2nm$, $P\bar{4}2_1m$, and $P4_2/mnm$ have mirror-plane symmetries imposing the orientation of the (BD_4) tetrahedron in such a way that the projections of the (BD_4) in the (001) plane are isocel triangles pointing in the direction defined by the projection of the Ca atoms aligned along the mirror planes in the (001) plane (see space groups $P4_2nm$ (no. 102), $P\bar{4}2_1m$, (no. 113), and $P4_2/mnm$ (no. 136)) in Figure 2). By contrast, $P4_2$ (no. 77), $P\bar{4}$ (no. 81)n and $P4_2/m$ (no. 84) do not have these symmetry constraints and have therefore a larger freedom of orientation of the (BD_4) in the (001) plane (see the three structures in Figure 2).

For tetrahydroborates, B−D distances for at least 1.0 Å are expected.[24–32] Except for the space group $P4_2$ and $P4_2/m$, all the other space groups give refined B−D distances significantly smaller than 1.0 Å. We observe a general trend of increasing displacement parameters with decreasing average B−D distances of the (BD_4) tetrahedron (see Table 4). This reflects the fact that models giving too-short B−D distances but a satisfying fit of the experimental data compensate for the wrong positions of D atoms by high displacement parameters. Accordingly, models with space group $P4_2$, $P\bar{4}$, and $P4_2/m$ having appropriate average bond lengths have significantly smaller displacement factors for D compared to the other models (however $P\bar{4}$ model, in spite of realistic average B−D distances, is strongly distorted, and some of its B−D distances are much smaller than 1.0 Å). Therefore, out of the seven structural-model candidates, only the two models with space groups $P4_2$ and $P4_2/m$ satisfy both appropriate bond length and reasonable amplitude of the displacement parameters (see Table 4).

In order to verify this result and find the optimal structural candidate, series of ab initio calculations were performed for the four structures showing refined (BD_4) with the most reasonable size and distortion (corresponding space groups are $P4_2$, $P4_2/m$, $P4_2nm$, $P\bar{4}n2$). An additional calculation was carried out for the space group $P4_2/mnm$, because it is a supergroup of all the seven other space-group candidates. The calculated electronic contribution to the formation energy indicates that structures with $P4_2nm$, $P\text{-}4n2m$, and $P4_2/mnm$ space groups have formation energies larger than $P4_2$ and $P4_2/m$ structures. Additionally, imaginary vibrational frequencies for these structures indicate their instability at finite temperatures (see Table 4). The $Ca(BD_4)_2$ in space groups $P4_2$ and $P4_2/m$ has the lowest formation energies, and all normal-mode frequencies are real positive, which indicates their stability at finite temperatures (see Table 4). This is in excellent agreement with experimental results. The B−H stretching normal-mode frequencies at the Γ point are in the range from 2341 to 2469 cm $^{-1}$ and from 2284 to 2455 cm $^{-1}$ for $P4_2$ and $P4_2/m$ structures, respectively. This frequency range of BH4 stretching is somewhat broader than that for other alkali tetrahydroborates,[27,32,33] and it compares

TABLE 5: Comparison of Selected Interatomic Distance Ranges (Å) of (BD_4) or (BH_4) tetrahedra for $Ca(BD_4)_2$ or $Ca(BH_4)_2$[a]

phase	T (K)	B−D	D−D	ΔB−D	ΔD−D
α	300	1.164(11)–1.174(11)	1.851(16)–1.965(14)	0.9	5.8
α[7]	300	1.107(2)–1.124(2)	1.723(1)–1.913(1)	1.5	9.9
α[b7]		1.229–1.240	1.973–2.055	8.9	4.0
β	480	1.02(3)–1.16(3)	1.63(3)–1.90(3)	12.1	14.2
β[b]		1.217–1.227	1.905–2.025	0.8	5.9
β[c]	480	1.06(3)–1.20(4)	1.50(5)–2.16(5)	11.7	30.6

[a] Difference between the two extreme values of each considered range Δ (%) is indicated. [b] Calculated. [c] Structural model with space group $P4_2$.

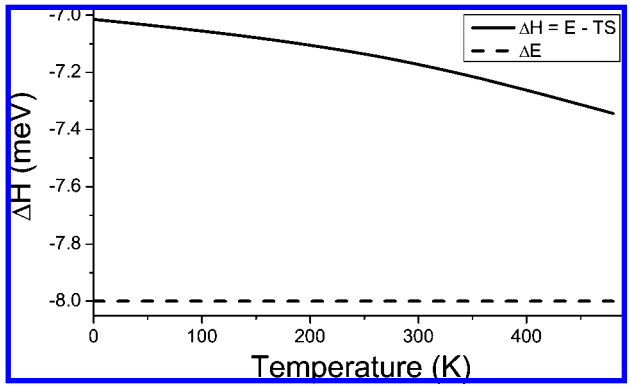

Figure 3. Calculated formation-energy difference between structural models with space group $P4_2/m$ (no. 84) and $P4_2$ (no. 77). Dotted line, electronic contribution of the formation energy ΔE; solid line, formation energy ΔH including zero-point energy and vibrational entropy.

within 5% with infrared and Raman spectroscopy data for $Ca(BH_4)_2$ recently reported in the literature.[5,34] We finally propose the structural model with space group $P4_2/m$ (see Table 2), because this space group has higher symmetry, lower formation energy, and more regular tetrahedrons (see Table 5) compared with the structural model with space group $P4_2$. The formation-energy difference, including vibrational entropy, between $P4_2/m$ and $P4_2$ structures is presented in Figure 3 and Table 4. However, disorder can be expected at a temperature of ∼480 K, as indicated by rather large displacement parameters of refined D atoms (see Table 2) and because it is observed in high-temperature modifications of other tetrahydroborates.[25–27,29,32,33,35] Therefore, considering the small formation-energy difference and the similar quality of fit between the model with space group $P4_2$ and $P4_2/m$ (see Table 4), we do not completely exclude the structural model with space group $P4_2$ (see Table 2).

The refined structure of the β phase of $Ca(BD_4)_2$ with $P4_2/m$ has Ca ions coordinated by six (BD_4) tetrahedra (see Figure 4) in a bidentate configuration. This is similar to the structure observed for the α phase where Ca ions are also coordinated by six (BD_4) tetrahedra (see Figure 5). The experimental (BD_4) geometry is slightly distorted with B−D interatomic distances in the range 1.02−1.16 Å. The D−D distances are in the range 1.63−1.90 Å (see Table 5). The differences between the experimental and calculated geometry could be due to disorder in the structure. The calculated (BD_4) geometry is closer to the ideal tetrahedral geometry with B−D interatomic distances in the range 1.217−1.227 Å and D−D distances in the range 1.905−2.025 Å (see Figure 4 and Table 5).

B. Orthorombic α-Phase Structure of $Ca(BD_4)_2$. In excellent agreement with the recently reported structural model of the α phase of $Ca(BD_4)_2$ at RT,[7] we found regular (BD_4) tetrahedron with B−D interatomic distances in the range 1.164−1.174 Å and D−D distances in the range 1.851−1.965(2) Å (see Figure 5 and Table 5). These values are slightly larger than the reported values obtained by using data from X-ray diffractometry and have a better agreement with the calculated values (see Table 5). The refined structure of the α phase of $Ca(BD_4)_2$ shows Ca ions coordinated with six (BD_4) tetrahedra (see Figure 5) in a bidentate configuration.

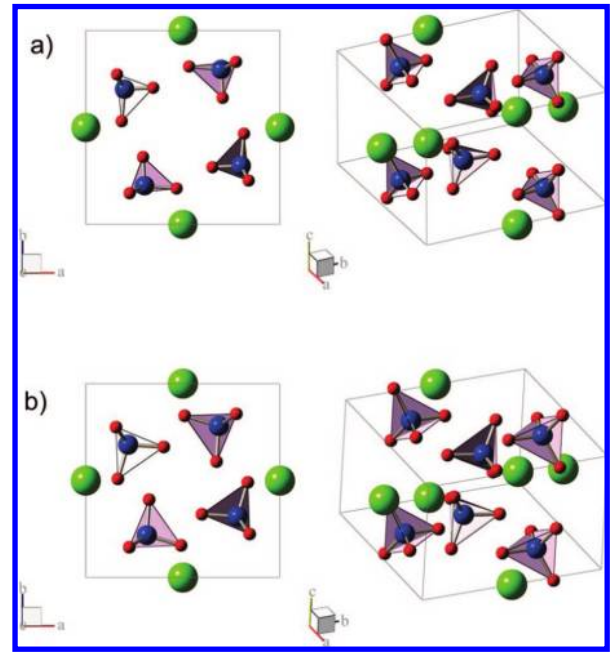

Figure 4. Structure of experimental and theoretical $Ca(BD_4)_2$ β phase. (a) Experimentaly refined structure. (b) Ab initio calculated structure.

The formation-energy calculations for the α phase indicate that the formation energy of the α phase is lower than that for the β phase but of the same order of magnitude, confirming that the α phase and the β phase of $Ca(BD_4)_2$ can be both present in the compound at the same thermodynamic conditions as it is observed in the sample synthesized by mechanochemical reaction or by the wet chemical chemistry method.

IV. Conclusion

A variety of coexisting modifications of $Ca(BD_4)_2$ were observed depending on the synthesis method and the temperature of the sample. Combining X-ray and neutron diffraction with ab initio calculations, we report on the solution and refinement of the β-phase crystal structure of $Ca(BD_4)_2$. We confirm the orthorombic crystal structure of the α phase recently reported for the corresponding hydride.[7] We indexed and found the space group of a hitherto unsolved γ phase of $Ca(BD_4)_2$.

Diffraction data was measured on a $Ca(BD_4)_2$ sample synthesized by solid−gas mechanochemical reaction by using MgB_2 as starting material. At RT, we observe this sample to be mostly in the α phase, and at ∼400 K, the sample transforms almost completely in the β phase. Diffraction data measured on this sample were used at RT to refine the α-phase structure, whereas above 400 K, diffraction data measured on the same sample were used to solve and refine the β phase. For the solution of the β phase, seven different structure candidates based on different tetragonal space groups were giving an equivalent quality of fit for both neutron and X-ray patterns. However, combined experimental and ab initio results have

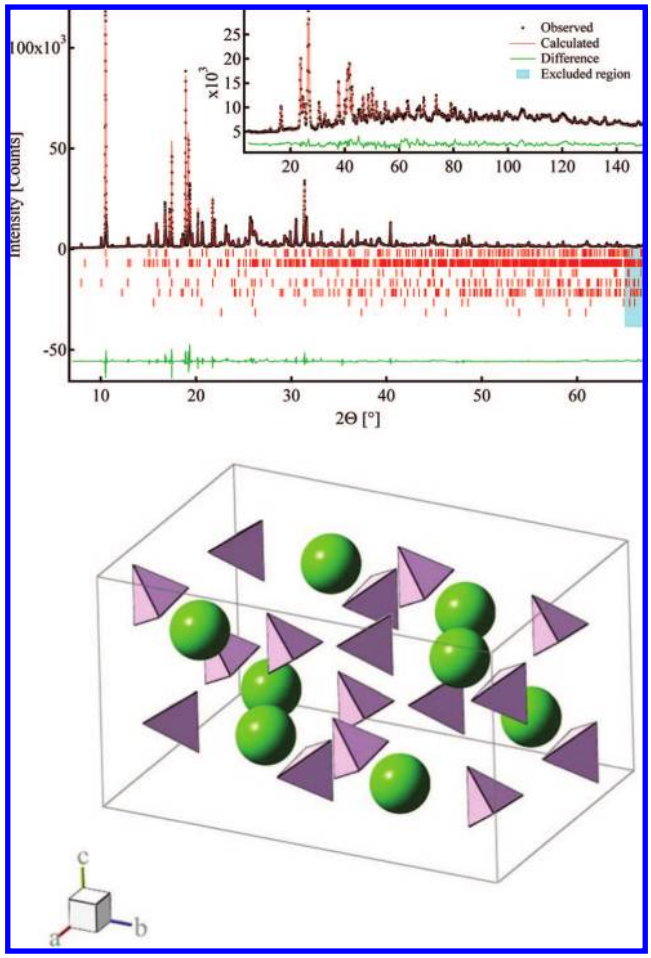

Figure 5. Result of combined SR-XPD and NPD (inset) Rietveld refinement of the $Ca(BD_4)_2$ α phase (only BD_4 shape and Li atom are drawed) by using diffraction patterns measured on the $Ca[^{11}BD_4]_2 + MgD_2$ sample at RT and corresponding structure. Rows of Bragg-peak positions are in the following order: α-$Ca(BD_4)_2$, γ-$Ca(BD_4)_2$, MgD_2, $Ca_4Mg_3D_{14}$, CaD_2, MgB_2, MgO, and V.

shown that the model with space group $P4_2/m$ is the best candidate that possesses appropriate size/geomery of the (BD_4) tetrahedron, lowest formation energy, and real positive vibrational energy, indicating a stable structure. In this sample, small amounts of γ phase were found to coexist with α phase at RT and with β phase at 480 K. Diffraction data were measured on a sample synthesized by the wet chemical method where the γ phase is present in a significant amount. This allowed us to index and determine a preliminar model of the γ phase with space group *Pbca* used to properly fit the diffraction data used to solve and refine the structure of the β phase.

Ab initio calculations of the α phase and the β phase of $Ca(BD_4)_2$ indicate similar energies of formation of all these structural phases (lower than 0.15 eV). These formation-energy differences are compatible with the presence of the different structural phases experimentally observed in the compound.

Acknowledgment. Support and skillful assistance from the team of the HRPT instrument (PSI, Villigen Switzerland), F. Gozzo at the SLS-MS beamline (PSI, Villigen, Switzerland), and H. Emerich and project team at the Swiss Norwegian Beam Line (ESRF, Grenoble France) is gratefully acknowledged. We are also gratefull to G. Vaughan and M. Brunelli for in-house beamtime and excellent assistance at ID31 beamline (ESRF, Grenoble France). CPU-time allocation at CSCS supercomputer center (Manno) is kindly acknowledged. Financial support by the Swiss National Science Foundation (Schweizerischer Nationalfonds, SNF), Projects no. 200020-115875 and no. 200021-119972/1 is gratefully acknowledged. Financial support by the European Commission DG Research (Contract SES6-2006-51827/NESSHY) and the Helmholtz Initiative FuncHy is gratefully acknowledged.

References and Notes

(1) Schlapbach, L.; Züttel, A. *Nature* **2001**, *414*, 353.
(2) Züttel, A.; Borgschulte, A.; Orimo, S. *Scr. Mater.* **2007**, *56*, 823.
(3) Orimo, S.; Nakamori, Y.; Eliseo, J. R.; Züttel, A.; Jensen, C. M. *Chem. Rev.* **2007**, *107*, 4111.
(4) Barkhordarian, G.; Klassen, T.; Dornheim, M.; Bormann, R. *J. Alloys Compd.* **2007**, *440*, L18.
(5) Barkhordarian, G.; Jensen, T. R.; Doppiu, S.; Bösenberg, U.; Borgschulte, A.; Gremaud, R.; Cerenius, Y.; Dornheim, M.; Klassen, T.; Bormann, R. *J. Phys. Chem. C* **2008**, *112*, 2743.
(6) Chłopek, K.; Frommen, C.; Léon, A.; Zabara, O.; Fichtner, M. *J. Mater. Chem.* **2007**, *17*, 3496.
(7) Miwa, K.; Aoki, M.; Noritake, T.; Ohba, N.; Nakamori, Y.; Towata, S.; Züttel, A.; Orimo, S. *Phys. Rev. B* **2006**, *74*, 155122.
(8) Riktor, M. D.; Sørby, M. H.; Chlopek, K.; Fichtner, M.; Buchter, F.; Züttel, A.; Hauback, B. C. *J. Mater. Chem.* **2007**, *17*, 4939.
(9) Filinchuk, Y.; Rönnebro, E.; Chandra, D.; submitted. Majzoub, E. H.; Rönnebro, E. submitted.
(10) David, W. I. F. Oral presentation, *International Symposium On Materials Issues In a Hydrogen Economy*, Richmond Virginia, 2007.
(11) Andresen, A. F.; Maeland, A. J.; Slotfeldt-Ellingsen, D. *J. Solid State Chem.* **1977**, *20*, 93.
(12) Kampel, V.; Warshawsky, A. *J. Organomet. Chem.* **1994**, *469*, 15.
(13) Boultif, A.; Louër, D. *J. Appl. Crystallogr.* **2004**, *37*, 724.
(14) Fischer, P.; Frey, G.; Koch, M.; Könnecke, M.; Pomjakushin, V.; Schefer, J.; Thut, R.; Schlumpf, N.; Bürge, R.; Greuter, U.; Bondt, S.; Berruyer, E. *Physica B* **2000**, *146*, 276–278.
(15) Favre-Nicolin, V.; Černý, R. *J. Appl. Crystallogr.* **2002**, *35*, 734.
(16) Rodríguez-Carvajal, J. *Physica B* **1993**, *192*, 55.
(17) Sears, V. F. *Neutron News* **1992**, *3*, 26.
(18) Kresse, G.; Furthmüller, J. *Comput. Mater. Sci.* **1996**, *6*, 15.
(19) Blöchl, P. E. *Phys. Rev. B* **1994**, *50*, 17953.
(20) Kresse, G.; Joubert, J. *Phys. Rev. B* **1999**, *59*, 1758.
(21) Bellaiche, L.; Kunc, K. *Phys. Rev. B* **1997**, *55*, 5006.
(22) Perdew, J. P.; Chevary, J. A.; Vosko, S. H.; Jackson, K. A.; Pederson, M. R.; Singh, D. J.; Fiolhais, C. *Phys. Rev. B* **1992**, *46*, 6671.
(23) Lodziana, Z.; Parlinski, K. *Phys. Rev. B* **2003**, *67*, 174106.
(24) Marynick, D. S.; Lipscomb, W. N. *Inorg. Chem.* **1972**, *11*, 820.
(25) Soulié, J.-Ph.; Renaudin, G.; Černý, R.; Yvon, K. *J. Alloys Compd.* **2002**, *346*, 200.
(26) Fischer, P.; Züttel, A. *Mater. Sci. Forum* **2004**, *287*, 443–444.
(27) Renaudin, G.; Gomes, S.; Hagemann, H.; Keller, L.; Yvon, K. *J. Alloys Compd.* **2004**, *375*, 98.
(28) Miwa, K.; Ohba, N.; Towata, S.; Nakamori, Y.; Orimo, S. *Phys. Rev. B* **2004**, *69*, 245120.
(29) Hartman, M.; Rush, J. J.; Udovic, T. J., Jr.; Hwang, S-J. *J. Solid State Chem.* **2007**, *180*, 1298.
(30) Cerny, R.; Filinchuk, Y.; Hagemann, H.; Yvon, K. *Angew. Chem., Int. Ed.* **2007**, *46*, 5765.
(31) Her, J.-H.; Stephens, P. W.; Gao, Y.; Soloveichik, G. L.; Rijssenbeek, J.; Andrus, M.; Zhao, J-C. *Acta Crystallogr., Sect. B: Struct. Sci.* **2007**, *63*, 561.
(32) Gomes, S.; Hagemann, H.; Yvon, K. *J. Alloys Compd.* **2002**, *346*, 206.
(33) Hagemann, H.; Gomes, S.; Renaudin, G.; Yvon, K. *J. Alloys Compd.* **2004**, *363*, 126.
(34) Fichtner, M.; Chłopek, K.; Longhini, M.; Hagemann, H. *J. Phys. Chem. C* **2008**, In press.
(35) Buchter F. To be published.

JP800435Z